



Effect of Nonlinear Thermal Radiation, Heat Source on MHD 3D Darcy-Forchheimer Flow of Nanofluid Over Aa Porous Medium with Chemical Reaction

Nainaru Tarakaramu¹, K. Ramesh Babu², P.V. Satyanarayana^{3,*}

¹ Department of Mathematics, School of Advanced Sciences, VIT, Vellore-632 014, T.N, India

² Department of Mathematics, Sree Vidyanikethan Engineering College (Autonomous), Tirupati-517102, A.P, India

³ Department of Mathematics, School of Advanced Sciences, VIT, Vellore-632 014, T.N, India

*Corresponding author E-mail: pvsatya8@yahoo.co.in

Abstract

The present work nonlinear thermal radiation and chemical reaction effect on three-dimensional MHD flow of permeable medium analysed. We are considering introduce the Darcy-Forchheimer law along with axial and transverse velocity. Using suitable transportations the nonlinear partial differential equations are converted into ordinary differential equations. These equations are solved numerically by 4th Runge-Kutta-Fehlberg scheme with shooting procedure. We are getting unique numerical solution for distinct physical variables temperature and concentration fields are depicted. Also the heat transfer and skin friction coefficients drawn through numerical data. We are finding great results of the velocity profiles behaviors opposite trend of porosity and Forchheimer parameters, the profiles of $\phi(\eta)$ and $\theta(\eta)$ behavior reverse trend follows other than chemical reaction parameter, both directions of skin friction coefficient and heat transfer rates reduction.

Keywords: Chemical reaction; Darcy-Forchheimer; Heat source; MHD; nonlinear Thermal radiation; Nanofluid; Porous medium.

1. Introduction

Current work investigation is most useful to ignore the higher velocity of fluid flow on sediments. These velocity reduction of the formula Darcy [1] was created a Darcy expression to describe the fluid flow in porous space. These theory mainly used to ignore the association of inertia and boundary influence. Present development world of high technology, the uses of porous media are characterized by more velocities. In generally, the flow of nonlinear is higher than the velocity of the fluid should be exist higher such type of effected on boundary layer and inertia can't be ignore under such conditions. To control this behavior is Darcy's expression, Forchheimer [2] expression added in the Darcy term by include the additional term of velocity square. This term is read as "Forchheimer term" which is applicable for higher Reynold rate. It has many applications in building thermal insulation materials, nuclear waste disposal, petroleum resources, energy storage units, solar receivers, heat exchanger, and beds of fossil fuels and so on. Mahammad et al [3] consider Darcy-Forchheimer term of 3D nanofluid flow on porous space. Hayat et al. [4] presented the 3D magnetohydrodynamic flow of an oldroyed -B nanofluid through stretching surface. Recently some of the scientists [5-6] investigated by Darcy-Forchheimer flow with heterogeneous-homogeneous effect. Hayat et al. [7] analyzed the convective boundary layer flow of viscous fluid with impact of carbon nanotubes. Harish babu et al. [8] create the magnetohydrodynamic Jeffrey fluid flow over stretching sheet with the effect of joule heating. Rana et al. [9] examine the nonaligned non-Newtonian flow non-linear thermal radiation.

The effect of Chemical reaction is great investigation area in biochemical engineering. It is done by several processes such as atmospheric flows, sinewy protection hydrometallurgical industry, ceramic and polymer production, synthetic handling, crop damage due to frost, and water and air pollutions and so on. Sadiq et al. [10] illustrated the chemical reaction on Maxwell fluid through stretchable flow. Ramzan et al. [11] developed the influence of chemical reaction, thermal radiation, and joule heating on Magneto-hydrodynamic nanofluid flow with gyrotactic microorganisms. Makinde et al. [12] examine the Magneto-hydrodynamic, thermal radiation, chemical reaction and homogeneous-heterogeneous effects on bioconvection nanofluid flow an upper surface of a paraboloid revolution. The chemical reaction effect on magneto-hydrodynamic Williamson nanofluid flow on permeable medium was examine Khan et al. [13]. Zhao et al. [14] investigated the effect of 1st order chemical reaction of magnetohydrodynamic flow on electrically conducting fluid b/w two infinite parallel plates. Mustafa et al. [15] analyzed the mixed convection flow of magnetohydrodynamic nanofluid flow on vertical stretching surface. Satya Narayana et al. [16] developed lie group analysis for the flow of heat transfer.

Fluid flow on permeable medium is studied a many applications in engineering and constructing. These flows are main role point in both natural and theoretical. Specific importance of this flow has been associated in thermal insulation process, chemical catalytic reactors, protection of gas cooled reactors, thermal energy usage, solar collectors and blood flow in lungs, thermal energy stockpiling forms, heat exchanger, and so on. The squeezed magnetohydrodynamic flow of water base fluids on porous has analyzed Kandasamy et al. [17]. Sivaraj et al. [18]. Developed the natural



convection in porous cavity with heat conducting solid body under the effect of magnetic field. Kandasamy et al. [19] explained the thermal properties compared to convective particle fluid suspension. Sudarsana Reddy et al. [20] developed heat and mass transfer of nanofluid flow on permeable medium with the effect of thermal radiation, magnetic field, and heat generation. Satynarayana et al. [21] examined the magnetohydrodynamic and heat transport flow of an Eyring-Powell fluid through stretching surface with the effect of viscous dissipation.

The theme of present study is to investigate the nonlinear thermal radiation, Heat source effects on three dimensional flow of MHD Darcy-Forchheimer nanofluid through stretching sheet with chemical reaction. The thermal conductivity of nanofluids are not constant and it varies linearly with the temperature. Similarity transformations are applied to nonlinear partial differential equations and the transformed system can be solved numerically by Runge-Kutta-Fehlberg scheme with shooting technique. Expressions for various values of parameters on the velocity and temperature as well as the skin friction coefficient and Nusselt number are discussed through graphically and numerically.

2. Mathematical Formulation

The impact of nonlinear thermal radiation on three-dimensional Darcy-Forchheimer nanofluid flow over porous medium with convective boundary condition. We choose 3D Cartesian coordinate variables u, v indicate as the direction system of x and y -direction are twofaced horizontal plane and fluid can be taken for $z = 0$. Nano-particles include steady nanofluid in the region of $z \geq 0$. Apply the effect of a constant magnetic field B_0 in the direction of z perpendicular to xy -plane. x, y -components corresponding to stretching velocity are u, v (here a, b are read as positive constants). In the direction of x surface of stretching with $a > 0$. The surface temperature is because of convective heating process which is featured by hot fluid temperature T_f and coefficient of heat transfer.

$$\frac{\partial u}{\partial x} + \frac{\partial v}{\partial y} + \frac{\partial w}{\partial z} = 0 \quad (1)$$

$$u \frac{\partial u}{\partial x} + v \frac{\partial u}{\partial y} + w \frac{\partial u}{\partial z} = \nu \left(\frac{\partial^2 u}{\partial z^2} \right) - \frac{\nu}{K} u - Fu^2 - \frac{\sigma B_0^2}{\rho} u \quad (2)$$

$$u \frac{\partial v}{\partial x} + v \frac{\partial v}{\partial y} + w \frac{\partial v}{\partial z} = \nu \left(\frac{\partial^2 v}{\partial z^2} \right) - \frac{\nu}{K} v - Fv^2 - \frac{\sigma B_0^2}{\rho} v \quad (3)$$

$$u \frac{\partial w}{\partial x} + v \frac{\partial w}{\partial y} + w \frac{\partial w}{\partial z} = \nu \left(\frac{\partial^2 w}{\partial z^2} \right) - \frac{\nu}{K} w - Fw^2 - \frac{\sigma B_0^2}{\rho} w \quad (4)$$

$$u \frac{\partial T}{\partial x} + v \frac{\partial T}{\partial y} + w \frac{\partial T}{\partial z} = \alpha_m \frac{\partial^2 T}{\partial z^2} - \frac{1}{(\rho C)_f} \frac{\partial q_r}{\partial z} + \frac{Q_0(T - T_\infty)}{(\rho c)_f} + \frac{(\rho C)_p}{(\rho C)_f} \left(D_B \frac{\partial T}{\partial z} \frac{\partial C}{\partial z} + \frac{D_T}{T_\infty} \left(\frac{\partial T}{\partial z} \right)^2 \right) \quad (5)$$

$$u \frac{\partial C}{\partial x} + v \frac{\partial C}{\partial y} + w \frac{\partial C}{\partial z} = \left(D_B \frac{\partial^2 C}{\partial z^2} + \frac{D_T}{T_\infty} \left(\frac{\partial T}{\partial z} \right)^2 \right) - K_0(C - C_\infty) \quad (6)$$

Where u, v and w are the variables of velocity components in direction of x, y and z respectively. Corresponding Boundary conditions are

$$\left. \begin{aligned} u = ax \quad v = by \quad w = 0, \\ -k_f \frac{\partial T}{\partial y} = h_f(T_f - T) \quad D_B \left(\frac{\partial C}{\partial z} \right) + \frac{D_T}{T_\infty} \left(\frac{\partial T}{\partial z} \right) = 0 \quad \text{at } z = 0 \\ u \rightarrow 0 \quad v \rightarrow 0 \quad T \rightarrow T_\infty \quad C \rightarrow C_\infty \quad \text{as } z \rightarrow \infty \end{aligned} \right\} \quad (7)$$

The radiative heat flux q_r which is given by Quinn Brewster (see ref. 22) is given by

$$\frac{\partial q_r}{\partial z} = -\frac{16\sigma^*}{3K^*} \frac{\partial}{\partial z} \left(T^3 \frac{\partial T}{\partial z} \right) \quad (8)$$

Substituting Eq. (8) in Eq. (5), we get below Expression

$$\left. \begin{aligned} u \frac{\partial T}{\partial x} + v \frac{\partial T}{\partial y} + w \frac{\partial T}{\partial z} = \alpha_m \frac{\partial^2 T}{\partial z^2} + \frac{1}{(\rho C)_f} \left(\frac{16\sigma^*}{3K^*} \frac{\partial}{\partial z} \left(T^3 \frac{\partial T}{\partial z} \right) \right) \\ + \frac{(\rho C)_p}{(\rho C)_f} \left(D_B \frac{\partial T}{\partial z} \frac{\partial C}{\partial z} + \frac{D_T}{T_\infty} \left(\frac{\partial T}{\partial z} \right)^2 \right) + \frac{Q_0(T - T_\infty)}{(\rho c)_f} \end{aligned} \right\} \quad (9)$$

The similarity transformations are

$$\left. \begin{aligned} \eta = \sqrt{\frac{a}{\nu_f}} z, \quad u = axf'(\eta), \quad v = ayg'(\eta), \\ w = -\sqrt{a\nu}(f + g), \quad \phi(\eta) = \frac{C - C_\infty}{C_\infty} \end{aligned} \right\} \quad (10)$$

Substituting Eq. (10) in Eqs. (2), (3), (4), (5) and (9) we get

$$f''' + f'(f + g)' - (1 + F_r)(f')^2 - (M + \lambda)f' = 0 \quad (11)$$

$$g''' + g'(f + g)' - (1 + F_r)(g')^2 - (M + \lambda)g' = 0 \quad (12)$$

$$\left(\frac{1 + R_d(\theta(\theta_w - 1) + 1)^3}{Pr} \right) \theta'' + N_b \theta' \phi' + N_t \theta'^2 + (f + g)\theta' = 0 \quad (13)$$

$$\phi'' + Sc\phi'(f + g)' + \theta'' \left(\frac{N_t}{N_b} \right) - \Gamma\phi = 0 \quad (14)$$

Corresponding boundary conditions as below:

$$\left. \begin{aligned} f = 0, \quad f' = 1, \quad g = 0, \quad g' = \lambda, \quad \theta' = -\gamma(1 - \theta) \\ N_b\phi + N_t\theta' = 0, \quad \text{at } \eta = 0 \\ f' \rightarrow 0, \quad g' \rightarrow 0, \quad \theta \rightarrow 0, \quad \phi \rightarrow 0, \quad \text{as } \eta \rightarrow \infty \end{aligned} \right\} \quad (15)$$

2.1 Appendix

$$\left. \begin{aligned} \Gamma = \frac{kv_f}{D_b a}, \quad F_r = \frac{C_b}{(K)^{1/2}}, \quad \lambda = \frac{\nu_f}{aK}, \quad Pr = \frac{\nu_f}{\alpha_m}, \quad N_b = \frac{(\rho C)_p D_T (T_f - T_\infty)}{(\rho C)_f \nu_f T_\infty} \\ N_t = \frac{(\rho C)_p D_C C_\infty}{(\rho C)_f \nu_f}, \quad Sc = \frac{\nu_f}{D_b}, \quad \gamma = \frac{h_f}{k_f} \left(\frac{\nu_f}{c} \right)^{1/2}, \quad \alpha = b/a \end{aligned} \right\} \quad (16)$$

Moreover the skin-friction coefficient and Nusselt number are below:

$$\left. \begin{aligned} \sqrt{\text{Re}_x} C_{fx} &= -f''(0), \quad \sqrt{\text{Re}_x} C_{fy} = -\alpha^{3/2} g''(0) \\ \frac{1}{\sqrt{\text{Re}_x}} Nu_x &= -(1 + R_d(\theta_w - 1) + 1)^3 \theta'(0) \end{aligned} \right\} \quad (17)$$

3. Results and Discussion

The transformed equations (11), (12), (13) and (14) with boundary conditions (15) has been solved numerically by Range-Kutta-Fehlberg method along with shooting technique. The graphical results are shown in Figures (2)-(15) for different parameters on the velocity and temperature profiles as well as the skin friction coefficient and Nusselt number.

The effects of λ , F_r , Γ , and H on $\phi(\eta)$ profile as depicted in Figs. 2-4. We have mainly noticed that the $\phi(\eta)$ profile increases with large ascending distinct values of porosity, Forchheimer and chemical reaction parameters, respectively while opposite trend follows the heat source parameter on $\phi(\eta)$ as depicted in Fig. 5. Physically, the thermophoresis force applicable highly in fluid flow on permeability the drives more particles settling to the stretching space so that concentration of heat generation/absorption.

The effects of F_r , λ on $\theta(\eta)$ profile as presented in Figs. 6 & 7. Here noticed that the $\theta(\eta)$ profile decreases with large distinct ascending numerical values of Forchheimer, porosity while increasing the chemical reaction parameter and heat generation parameter on $\theta(\eta)$ as depicted in Figs. 8-9. Physically, the temperature difference exists high then the thermophoresis force applicable highly in fluid flow on permeability, the particles closed to the stretching space so that temperature of chemical reaction Γ and heat generation/absorption H increases.

The effects of R_d on $\theta(\eta)$, $\phi(\eta)$ profile as presented in Figs. 10-11. It is noticed that the $\theta(\eta)$ profile decreases with large distinct ascending numerical values of R_d . Because, radiation is inversely proportional to thermal diffusivity, which is produce weaker thermal diffusivity. Such diffusivity yield an escalating temperature. While opposite direction follows R_d on $\phi(\eta)$. Because, low molecular diffusion on concentration and boundary layer thickness as plotted in Fig. 11.

The effects of θ_w on $\theta(\eta)$, $\phi(\eta)$ profile as presented in Figs. 12-13. We have seen that the $\theta(\eta)$ profile decreases with large distinct ascending numerical values of θ_w . Physically, temperature ratio is proportional to ambient temperature of the fluid, which is produce high temperature. Such ambient temperature yield an enhancement temperature. While opposite direction follows θ_w on $\phi(\eta)$ and associated boundary layer thickness as explored in Figure. 13.

In Figs. 14 & 15 shows that the variation between the effects of F_r with respect to λ on $\text{Re}_x^{1/2} C_{fx}$, $\text{Re}_y^{1/2} C_{fy}$ along x , y direction respectively. It is noticed that both $\text{Re}_x^{1/2} C_{fx}$, $\text{Re}_y^{1/2} C_{fy}$ profiles decreases with large distinct ascending numerical values of Forchheimer F_r . Physically, the Reynolds rate decreases in fluid flow on permeability medium for applicable of law of Darcy so that the mass transfer can be decreases. In Fig. 16 shows that the variation between the effects of F_r with respect to R_d on $\text{Re}_x^{-1/2} Nu_x$. Here

noticed that $\text{Re}_x^{-1/2} Nu_x$ decreases with large ascending values of Forchheimer F_r .

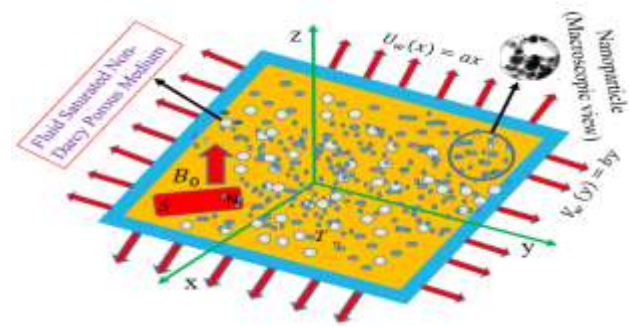


Fig. 1: Flow configuration and coordinate system.

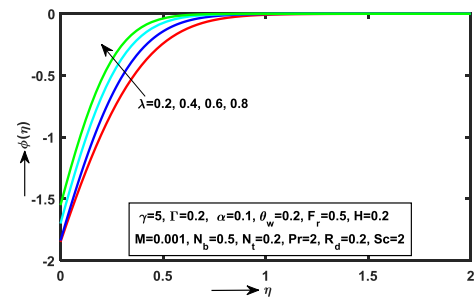


Figure 2 Influence of λ on $\phi(\eta)$

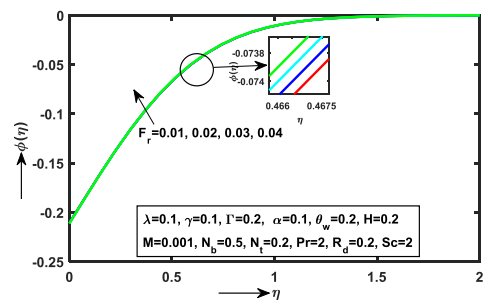


Fig. 3: Influence of F_r on $\phi(\eta)$

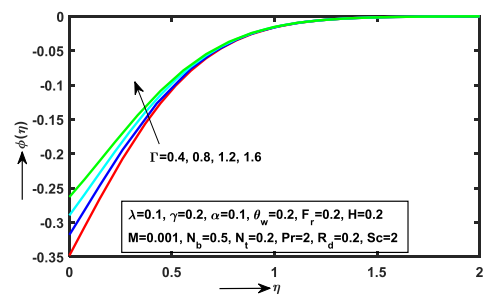


Fig. 4: Influence of Γ on $\phi(\eta)$

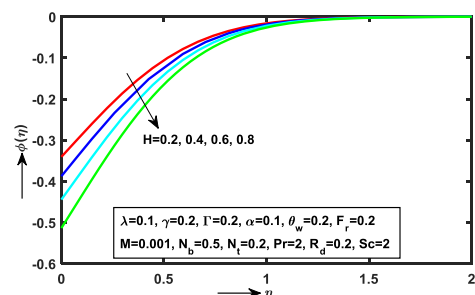


Fig. 5: Influence of H on $\phi(\eta)$

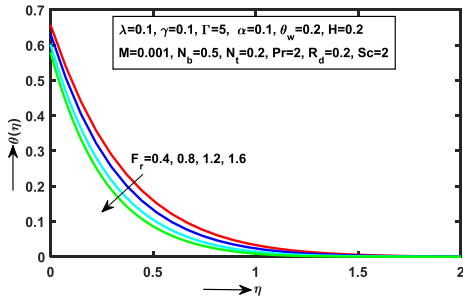


Fig. 6: Influence of F_r on $\theta(\eta)$

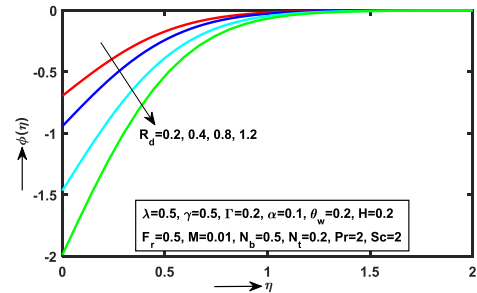


Fig. 11: Influence of R_d on $\phi(\eta)$

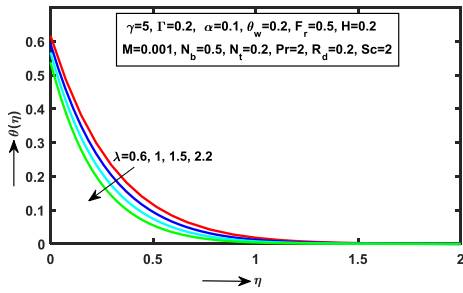


Fig. 7: Influence of λ on $\theta(\eta)$

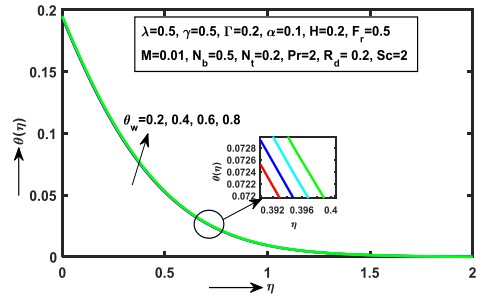


Fig.12: Influence of θ_w on $\theta(\eta)$

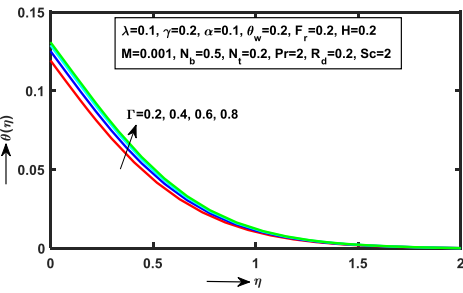


Fig. 8: Influence of Γ on $\theta(\eta)$

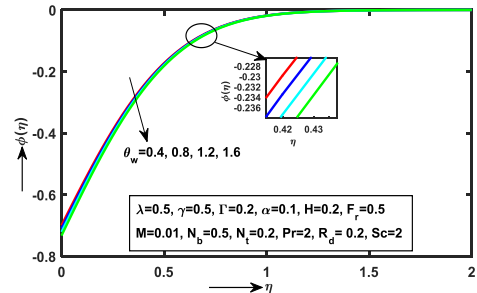


Fig. 13: Influence of θ_w on $\phi(\eta)$

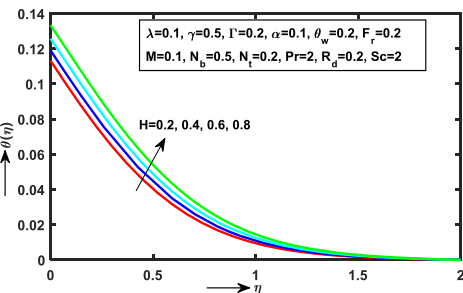


Fig. 9: influence of H on $\theta(\eta)$

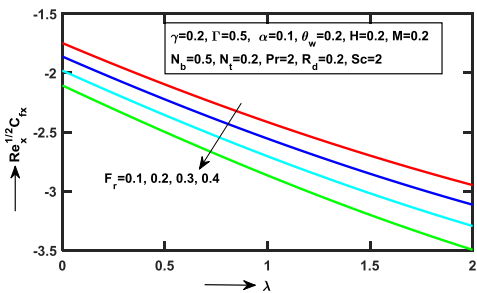


Fig. 14: Variation of F_r on $Re_x^{1/2} C_{fx}$ against λ

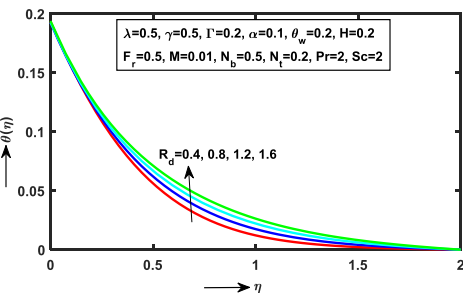


Fig. 10: Influence of R_d on $\theta(\eta)$

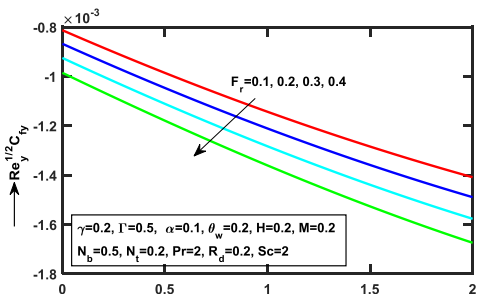


Fig. 15: Variation of F_r on $Re_y^{1/2} C_{fy}$ against λ

4. Conclusion

The present analysis thermal radiation effect on 3D MHD Darcy-Forchheimer flow of nanofluid with chemical reaction and convective condition. Here we are found that unique results are declared as follows:

- ❖ The velocity of effected parameters F_r and λ are opposite trend along axial and transverse direction.
- ❖ The impact of F_r , λ and Γ are decreasing on $\phi(\eta)$ while opposite trend behaviour follows on $\theta(\eta)$ profile with distinct ascending values of F_r .
- ❖ The enhancement profile $\theta(\eta)$ for given distinct values of R_d , θ_w respectively, while reverse trend follows the concentration boundary layer.
- ❖ The skin friction coefficient along $Re_x^{1/2} C_{fx}$, $Re_y^{1/2} C_{fy}$ and heat transfer dwindle with ascending values of F_r .

References

- [1]. Darcy H (1856), Les fontaines publiques de la ville de Dijon, *Victor Dalmont, Paris*.
- [2]. Forchheimer P (1901), Wasserbewegung durch boden, *Zeitschrift, Ver D. Ing.* 45, 1782–1788.
- [3]. Mahammad T, Alsaedi A, Shehzad SA, Hayat T, (2017), A revised model for Darcy-Forchheimer flow of Maxwell nanofluid subject to convective boundary condition. *Chines Journal of Physics*, 55, 963-9.
- [4]. Hayat T, Qayyum S, Shehzad SA, Alsaedi A (2017), Magneto-hydrodynamic three-dimensional nonlinear convection flow of Oldroyd-B nanofluid with heat generation/absorption, *J. Mole. Liq.* 230, 641–651.
- [5]. Hayat T, Haider F, Muhammad T, Alsaedi A (2017), Darcy-Forchheimer flow with cattaneo-christov heat flux and homogeneous heterogeneous reactions, *PLOS ONE*, 12, 4, 1-18.
- [6]. Hayat T, Shah F, Alsaedi A, Khan MI (2017), Development of homogeneous/heterogeneous reaction in flow based through non-Darcy Forchheimer medium, *J. Theoretical Comp. Chem.* 16, 5, 1-21.
- [7]. Hayat T, Khan MI, Farooq M, Alsaedi A, Yasmeen T (2017), Impact of Marangoni convection in the flow of carbon-water nanofluid with thermal radiation, *Int. J. Heat Mass Transfer*, 106,810–815
- [8]. Harish Babu D, Satya Narayana PV (2016), Joule heating effects on MHD mixed convection of a Jeffrey fluid over a stretching sheet with power law heat flux: A Numerical Study, *J. Magn. Magnet. Mater.* 412,185-193.
- [9]. Rana S, Mehmood R, Narayana PVS, Akbar NS (2016), free convective nonaligned non-Newtonian flow with non-linear thermal radiation, *Commun. Theor. Phys.* 66, 687–693.
- [10]. Sadiq MA, Waqas M, Hayat T (2017), Importance of Darcy-Forchheimer relation in chemically reactive radiating flow towards convectively heated surface, *J. Mole. Liq.* 248, 1071–1077.
- [11]. Ramzan M, Chung JD, Ullah N (2017), Radiative magnetohydrodynamic nanofluid flow due to gyrotactic microorganisms with chemical reaction and non-linear thermal radiation, *Int. J. Mech. Sci.* 130, 31–40.
- [12]. Makinde OD, Animasaun IL (2016), Bioconvection in MHD nanofluid flow with nonlinear thermal radiation and quartic autocatalysis chemical reaction past an upper surface of a paraboloid of revolution, *Int. J. Thermal Sci.* 109, 159-171.
- [13]. M. Khan, M.Y. Malik, T. Salahuddin, Rehman KU, Naseer M, Khan I (2017), MHD flow of Williamson nanofluid over a cone and plate with chemically reactive species, *J. Mole. Liq.* 231, 580–588.
- [14]. Zhao Q, Xu H, Tao L (2017), Unsteady bioconvection squeezing flow in a horizontal channel with chemical reaction and magnetic field effects, *Math. Problems Eng.* 1-10. <https://doi.org/10.1155/2017/2541413>.
- [15]. Mustafa M, Khan JA, Hayat T (2017), Alsaedi A, Buoyancy effects on the MHD nanofluid flow past a vertical surface with chemical reaction and activation energy, *Int. J. Heat Mass Transfer*, 108, 1340–1346.
- [16]. Satya Narayana PV (2017), Lie group analysis for the flow and heat transfer of a nanofluid over a stretching sheet with viscous dissipation, *J. Nanofluids*, 6, 1181-1187.
- [17]. Kandasamy R, Mohammad R, Zailani NABM, Jaafar NFB (2017), Nanoparticle shapes on squeezed MHD nanofluid flow over a porous sensor surface, *J. Mole. Liq.* 233, 156–165.
- [18]. Sivaraj C, Sheremet MA (2017), MHD natural convection in an inclined square porous cavity with a heat conducting solid block, *J. Magn. Magnet. Mater.* 426, 351–360.
- [19]. Kandasamy R, Dharmalingam R, Sivagnana Prabhu KK (2017), Thermal and solutal stratification on MHD nanofluid flow over a porous vertical plate, *Alexandria Eng. J.* 1-10.
- [20]. Sudarsana Reddy P, Chamkha AJ, Mudhaf AA (2017), MHD heat and mass transfer flow of a nanofluid over an inclined vertical porous plate with radiation and heat generation/absorption, *Advanced Powder Tech.* 28, 1008–1017.
- [21]. Satya Narayana PV, Tarakaramu N, Akshith SM, Ghori JP (2017), MHD flow and heat transfer of an Eyring - Powell fluid over a linear stretching sheet with viscous dissipation - a numerical study, *Frontiers Heat Mass Transfer*, 9, 9, 1-5.
- [22]. Brewster MQ (1972), Thermal radiative transfer properties, Wiley, New York.